Available online at www.sciencedirect.com
ScienceDirect
Chemical Physics Letters 435 (2007) 182–187
CHEMICAL PHYSICS LETTERS
www.elsevier.com/locate/cplett

Symmetry and vibrationally resolved absorption spectra near the O K edge of N_2O: Experiment and theory

T. Tanaka [a], K. Ueda [b,1], R. Feifel [b,c,*], L. Karlsson [c], H. Tanaka [a], M. Hoshino [a], M. Kitajima [d], M. Ehara [e], R. Fukuda [e,f], R. Tamaki [e], H. Nakatsuji [e,f]

[a] *Department of Physics, Sophia University, Tokyo 102-8554, Japan*
[b] *Institute of Multidisciplinary Research for Advanced Materials, Tohoku University, Sendai 980-8577, Japan*
[c] *Department of Physics, Uppsala University, Box 530, SE-751 21 Uppsala, Sweden*
[d] *Tokyo Institute of Technology, Tokyo 152-8551, Japan*
[e] *Department of Synthetic Chemistry and Biological Chemistry, Graduate School of Engineering, Kyoto University, Katsura Nishikyo-ku, Kyoto 615-8510, Japan*
[f] *Quantum Chemistry Research Institute, 58-8 Mikawa, Momoyama-cho, Fushimi-ku, Kyoto 612-8029, Japan*

Received 17 November 2006; in final form 13 December 2006
Available online 28 December 2006

Abstract

Angle-resolved energetic-ion yield spectra have been measured in the O 1s excitation region of N_2O. Franck–Condon analysis based on *ab initio* two-dimensional potential energy surfaces of the core-excited Rydberg states reproduces well the observed vibrational excitations specific to the individual Rydberg states. The irregular Rydberg behavior in the Σ-symmetry absorption spectrum is attributed the valence-Rydberg coupling in light of the second moment analysis.

1. Introduction

Inner-shell absorption spectroscopy is often performed today at high-flux and high-resolution synchrotron radiation beam lines in succession to the original electron-energy-loss spectroscopy (EELS) technique [1]. It gives important information on the electronic structure and nuclear dynamics of core-excited species [2]. In the case of randomly-oriented free molecules, the drawback of *traditional*, i.e. angle-integrated, EELS and photoabsorption spectroscopy is that they are insensitive to the symmetries of the excited electronic states, which information is often vital for making unambiguous assignments, in particular if several electronic states overlap or even coincide. A breakthrough for gas phase soft X-ray absorption spectroscopy in this respect has been the introduction of angle-resolved yield measurements of fragment ions of inner-shell excited linear molecules [3–6]. Within the validity of the axial-recoil approximation [7,8], which assumes the dissociation rate to be much faster than the molecular rotational period, symmetry information can be extracted for linear molecules from this technique according to following principle: for absorption transitions of $\Delta\Lambda = 0$ (i.e. $\Sigma \rightarrow \Sigma$, $\Pi \rightarrow \Pi$, etc.), fragment ions are preferentially detected parallel to the direction of the electric field vector of the linear polarized light, whereas for absorption transitions of $\Delta\Lambda = \pm 1$ (i.e. $\Sigma \rightarrow \Pi$, $\Pi \rightarrow \Sigma$, etc.), fragment ions are preferentially detected perpendicular to the direction of the electric field vector. This method is therefore often referred to 'symmetry-resolved' absorption spectroscopy [6,9].

The N_2O molecule studied here has two inequivalent nitrogen atoms, the terminal N_t and the center N_c, in a

* Corresponding author. Address: Department of Physics, Uppsala University, Box 530, SE-751 21 Uppsala, Sweden. Fax: +46 18 471 3524.
E-mail addresses: ueda@tagen.tohoku.ac.jp (K. Ueda), raimund.feifel@fysik.uu.se (R. Feifel).
[1] Fax: +81 22 217 5380.

0009-2614/$ - see front matter © 2006 Elsevier B.V. All rights reserved.
doi:10.1016/j.cplett.2006.12.071

linear geometry in the neutral ground state, and its electronic configuration can be denoted as

$$(1\sigma)^2(2\sigma)^2(3\sigma)^2(4\sigma)^2(5\sigma)^2(6\sigma)^2(1\pi)^4(7\sigma)^2(2\pi)^4(^1\Sigma^+),$$

where 1σ, 2σ and 3σ correspond to the O 1s, N_c 1s, and N_t 1s core orbitals, respectively. The N_2O molecule has four vibrational modes, two stretching modes $(v_1', 0, 0)$ and $(0, 0, v_3')$ and a doubly-degenerate bending mode $(0, v_2', 0)$. $(v_1', 0, 0)$ and $(0, 0, v_3')$ are similar to symmetric and antisymmetric vibrations, respectively, in CO_2, and thus are often called quasi-symmetric and quasi-antisymmetric stretching vibrations, respectively.

Adachi et al. [10] presented the first angle-resolved energetic-ion yield (ARIY) spectra of N 1s and O 1s excited N_2O, and investigated them with the help of *ab initio* quantum mechanical calculations. They paid special attention to the O 1s, N_c 1s, and N_t 1s → π* excitations and showed that Renner–Teller coupling via the $(0, v_2', 0)$ mode is present in all three of them, which breaks the degeneracy of these states by bending the linear molecule. More recently, Tanaka et al. [11] found that the Renner–Teller effect in these three Π states is even more pronounced in a hot target gas compared to N_2O molecules at room-temperature. The work of Adachi et al. [10] further showed that no Renner–Teller effect is present in any of the 1s → Rydberg excited states, which suggests that the axial-recoil approximation is fully valid in these cases, and which allows one to obtain reliable symmetry information from ARIY measurements in the corresponding spectral regions. Prince et al. [12] recorded recently near-edge total yield X-ray absorption fine structure spectra, without symmetry-resolution, but at high energy resolution near both the N 1s and O 1s edges of N_2O: several new Rydberg states converging to the oxygen K-edge including some overlapping vibrational structures were revealed in their study.

In the present work, we applied symmetry-resolved X-ray absorption spectroscopy to the O 1s → Rydberg excitation in the N_2O molecule. Utilizing both high energy resolution and symmetry resolution allow us to observe state-specific vibrational structures for the individual symmetry-resolved electronic states. The vibrational structures are theoretically examined based on a Franck–Condon (FC) analysis using *ab initio* two-dimensional (2D) potential energy surfaces (PES). For the calculation of the 2D PES of core-excited states, the symmetry-adapted-cluster configuration-interaction (SAC–CI) method [13–17] is adopted within the equivalent core model (ECM). The ECM has been used previously for the analysis and simulations of the vibrational spectra that appear in the core-hole states [18–21].

2. Experimental

The experiments were performed at the c-branch of the photochemistry beam line 27SU [22] at SPring-8, Japan, which is equipped with a high-resolution varied-line space soft X-ray monochromator [23]. The radiation source is a figure-8 undulator which can provide either horizontally or vertically linear polarized light by setting the undulator gap appropriately [24]. Two ion detectors, to each of which a retarding potential of +6 V is applied for detecting ions with kinetic energies higher than 6 eV, are mounted at 0° and 90° with respect to the electric field vector of the synchrotron light [2,25]. They were used for recording the symmetry-resolved near-edge X-ray absorption fine structure spectra. The acceptance angle for fragment ions in the detectors is about ±9°, and the ratio of the detection efficiencies of the two detectors, needed for calibrating them identically, was determined by comparing the ARIY spectra recorded using horizontally and vertically linear polarized light. A 4π-sr ion detector is placed 250 mm away from the other two detectors and has been used to record the total ion yield (TIY) simultaneously with the ARIYs. The photon energy bandwidth of the monochromator was set to 50 meV for the O 1s excitation region. The monitor of the photon flux for the normalization was made by a drain current after the gas sample. All spectra are normalized to the data acquisition time, the gas pressure and the photon flux. The photon energy scale was calibrated using the TIY spectra of Prince et al. [12] as reference. N_2O gas was commercially obtained with a stated purity of >99.99%.

3. Theoretical

2D PESs of the ground and O 1s core-excited states were calculated along the direction of the normal coordinates q_1 and q_3 corresponding to the quasi-symmetric (v_1') and quasi-antisymmetric (v_3') stretching vibrational motions, respectively, in the regions of $R_{NN} = 1.00$–1.30 Å and $R_{NO} = 1.05$–1.55 Å. The ground-state geometry is calculated to be $R_{NN} = 1.122$ and $R_{NO} = 1.184$ Å, in good agreement with the experimental values [26] of 1.127 and 1.185 Å, respectively. To calculate the 2D PES of the core-excited states, the ECM was adopted. For the O 1s excited state, the excited states of NNF were calculated by the SAC–CI method. The basis sets were correlation consistent polarized valence triple zeta (cc-pVTZ) basis sets proposed by Dunning, namely [4s3p2d] [27] plus Rydberg functions [5s5p5d] [28] placed on the center N atom for describing $n = 3, 4, 5$ (s, p, d). SAC–CI SD-*R* calculations were performed and the excited states of the neutral radical NNF were calculated by electron attachment to NNF^+. The SAC–CI SD-*R* method, in which single (S) and double (D) excitations are adopted for *R*-operators, is useful for calculating one-electron processes. We employed the algorithm calculating σ-vectors directly, which includes all the non-linear terms [29]. All the *R*-operators were included without selection in the SAC–CI calculations, while the perturbation selection procedure was adopted for the SAC calculations with the energy threshold of $\lambda_g = 10^{-6}$ au to reduce the computational requirements [30].

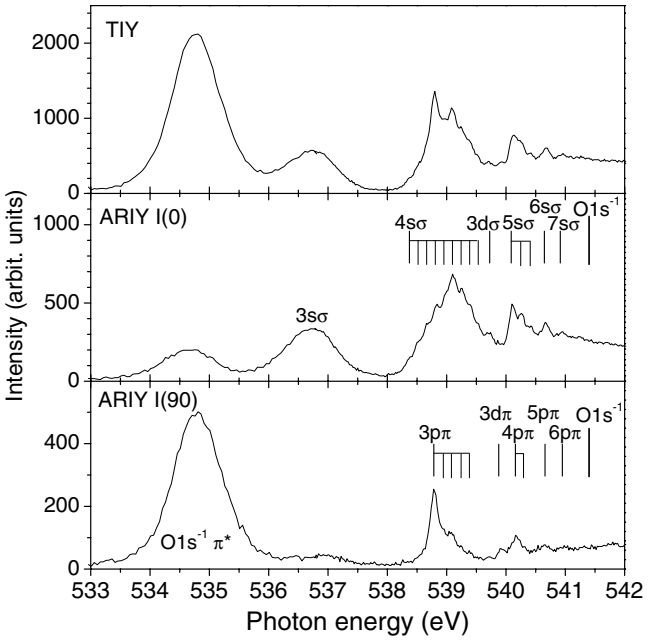

Fig. 1. High resolution oxygen K-edge total ion yield (TIY) and angle-resolved energetic-ion yield (ARIY) spectra of N_2O recorded in the photon energy range between 533 and 542 eV. Upper panel: TIY spectrum; middle panel: ARIY spectrum of the Σ-symmetry channel ($\Delta\Lambda = 0$); lower panel: ARIY spectrum of the Π-symmetry channel ($\Delta\Lambda = 1$). Teeth of the comb represent the vibrational components experimentally observed and are listed in Table 1.

The calculated PESs were fitted with two dimensional Morse functions and a vibrational analysis was performed. For calculating the spectrum, vibrational wave functions and the FC factors (FCF) were obtained by the grid method, in which Lanczos algorithm was adopted for the diagonalization. The SAC–CI calculations were performed with the development version of the GAUSSIAN 03 suite of programs [31].

4. Results and discussion

In Fig. 1 we present the TIY (upper panel) and ARIY (I(0°) middle panel; I(90°) lower panel) spectra of N_2O recorded in the photon energy region between 533 and 542 eV. The O 1s ionization threshold, located at 541.4 eV [12], serves as a reference mark for the assignments of the various spectral features discernable in this figure. The assignments are summarized in Table 1 together with the results of Adachi et al. [10] and Prince et al. [12] for comparison.

The broad features centered around 534.8 eV and 536.8 eV photon energies in the TIY spectrum are the O $1s^{-1}\pi^*$ and O $1s^{-1}3s\sigma$ resonances [9–12], respectively. The former one is also present in the 0° measurements where its maximum is shifted by about 0.1 eV towards lower photon energy due to the Renner–Teller effect as discussed in detail by Adachi et al. [9,10].

Table 1
Energies, assignments and quantum defects δ for the Rydberg states identified in the angle-resolved energetic-ion yield spectra of Fig. 1

Experiment (eV)	Theory (eV)	Assignment	δ	Prince [12]	Adachi [10]
534.66		π^* bent A_1			
534.76		π^* linear B_1		π^*	π^*
536.71		3sσ		3sσ	3sσ
538.38	538.38	4sσ	1.88	4sσ	
538.52	538.52	4sσ(100)		4sσ(001)	
538.66	538.66, 538.67	4sσ(200)/(001)		4sσ(100)	
538.78	538.78	3pπ	0.72	3pπ + 4sσ(101)	3pπ
538.82	538.79, 538.81	4sσ(300)/(101)			
538.94	538.91	3pπ(100)			
538.98	538.92, 538.95, 538.96	4sσ(400)/(201)/(002)		3pπ(001) + 4sσ(200)	
539.08	539.03, 539.08	3pπ(200)/(001)			
539.10	539.05, 539.08, 539.10	4sσ(500)/(301)/(102)		4sσ(201) + 3pπ(002)	4sσ
539.24	539.21	3pπ(101)		4sσ(202) + 3pπ(002)	
539.25	539.21, 539.24, 539.25	4sσ(401)/(202)/(003)		4sσ(202) + 3pπ(002)	
539.38	539.34, 539.38	3pπ(201)/(002)			
539.40	539.34, 539.37, 539.39	4sσ(501)/(302)/(103)			
539.52	539.46, 539.50, 539.53	4sσ(601)/(402)/(004)			
539.72		3dσ	0.15	3dσ	
539.90		3dπ	−0.01	3dπ	3dπ
540.10		5sσ	1.77	4pπ/5sσ	4pπ
540.16		4pπ	0.69		
540.26		5sσ(100)		5sσ(001)	5sσ
540.32		4pπ(100)			
540.40		5sσ(100)/4dσ		5sσ(100)	
540.64		5pπ	0.77	5pπ + 5sσ(200)	5pπ
540.66		6sσ	1.71	5pπ + 5sσ(200)	
540.96		7sσ	1.44	5sσ(300)	
540.98		6pπ	0.31		

Theoretical values are given for the peaks of the 4sσ and 3pπ states whose FCF is larger than 0.015.

The TIY recording shows a comparatively broad feature around 539 eV photon energy, with two distinct peaks on top of it at 538.80 and 539.10 eV. As can be seen from the middle and lower panel of Fig. 1, the peak at 538.80 eV belongs to a state of Π-symmetry and the other one at 539.10 eV to a state of Σ-symmetry. Adachi et al. assigned the state at 538.80 eV to the O $1s^{-1}3p\pi$ Rydberg state [9,10]. In the ARIY (I(90°)) recording, we can see well resolved vibrational fine structure, with spacings of 0.14–0.16 eV, of this state. The non-Poisson intensity distribution suggests two vibrational modes $(v_1,0,v_3)$ to be active. The state centered around 539.10 eV photon energy corresponds to a broad band in the ARIY (I(0°)) recording. This band is associated with the O $1s^{-1}4s\sigma$ Rydberg state [10], and it shows also some vibrational fine structure, with spacings of 0.12–0.16 eV, as shown in Fig. 1. Again the non-Poisson intensity distribution suggests two vibrational modes $(v_1,0,v_3)$ to be active.

The sharp spectral features observed above 540 eV photon energy in the TIY recording decompose into states of Σ- and Π-symmetry channels, as revealed in the ARIY (I(0°)) and ARIY (I(90°)) recordings, and can be assigned to higher members of the $ns\sigma$ and $np\pi$ Rydberg series, respectively, according to their apparent quantum defects. For the $7s\sigma$ and $6p\pi$ states the quantum defects deviate somewhat from the values of their respective series. This behaviour does not influence the interpretations but is rather a result of low accuracy in the energy measurements.

It is of particular interest to notice that vibrational fine structures are state-specific. The $3s\sigma$ state exhibits no vibrational structure indicating the dissociative nature of the state. A long vibrational progression of the $4s\sigma$ state illustrates large geometry relaxation of this state. The vibrations are less excited in the $5s\sigma$ state, indicating the small geometry relaxation of this state. The Π-channel, on the other hand, does not show such distinct vibrational excitations.

In order to understand this state-specificity of vibrational excitations, we have performed FC analysis based on *ab initio* 2D PESs, using the SAC–CI-ECM method described in Section 3. Fig. 2a and b illustrate the cut of 2D PESs with $R_{NN} = 1.10$ Å for the core-excited states belonging to the Σ-, Δ- and Π-symmetry channels, respectively. The 2D PESs of $nl\pi$ Rydberg states are nearly parallel to the ionized state. The FC analysis of the $3p\pi$ state reproduces well the vibrational structure observed in the O $1s \rightarrow 3p\pi$ excitation spectrum, as shown in Fig. 3b, and confirms the reliability of the calculated 2D PESs. The assignments of the individual bars in Fig. 3b are also given in Table 1, where the scale of the theoretical energies is shifted so that the energy of the vibrational ground state (0,0,0) coincides with the experimental one. It is clear from the calculations that the observed vibrational structure consists of the progressions $(v_1,0,0)$ and $(v_1,0,1)$. The 2D PES of the $3s\sigma$ state appears to be dissociative and thus explains the fact that there is no vibrational structure in the excitation spectrum in Fig. 1. The 2D

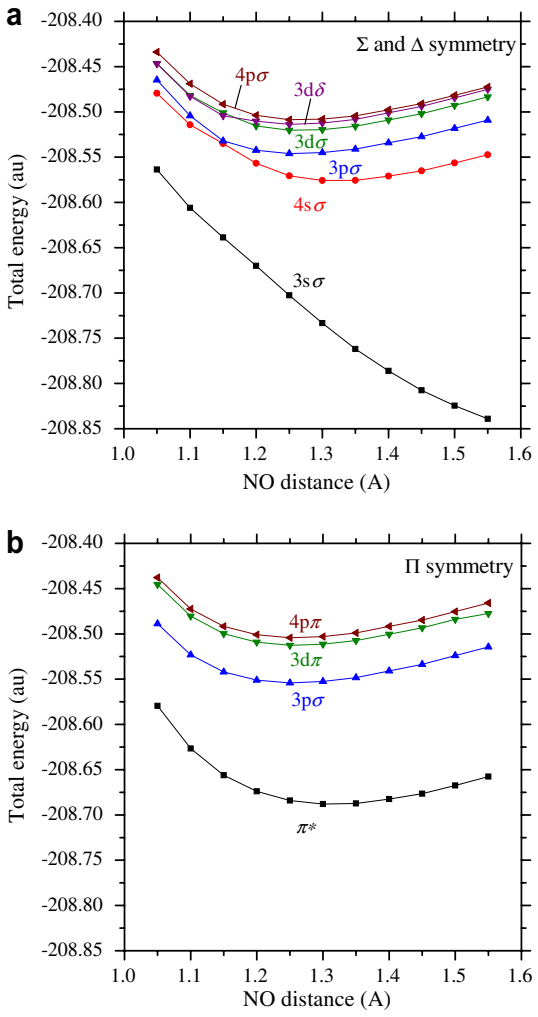

Fig. 2. Adiabatic potential energy curves of the low-lying O 1s excited states in (a) Σ-, Δ- and (b) Π-symmetry with the cut of $R_{NN} = 1.10$ Å.

PES of the $4s\sigma$ state shows large geometry relaxation relative to the neutral ground state and hence can explain the observed long vibrational progression. Indeed, the FC analysis of the $4s\sigma$ state reasonably reproduces the observed vibrational structure, as shown in Fig. 3a. In the calculation in Fig. 3a, only the $4s\sigma$ band is included. According to the potential curves in Fig. 2a, the $3p\sigma$ band may overlap with the higher energy side of the $4s\sigma$ band. The assignments of the individual bars in Fig. 3a are also given in Table 1. According to the calculations, not only the $(v_1,0,0)$ components but also all the $(v_1,0,v_3)$ components are excited. For higher $nl\sigma$ members, the 2D PESs are nearly parallel to the ionized state, and therefore explain the observation that the vibrational excitations are similar to that of $3p\pi$.

The origin of the significant change of the vibrational structures observed in the Σ-symmetry channel can be found in the valence-Rydberg coupling in this channel. We expect that the σ^* valence state is strongly mixed in the $ns\sigma$ Rydberg states [10] and perturbs the regular Rydberg behavior of the PESs. In order to estimate the effect of

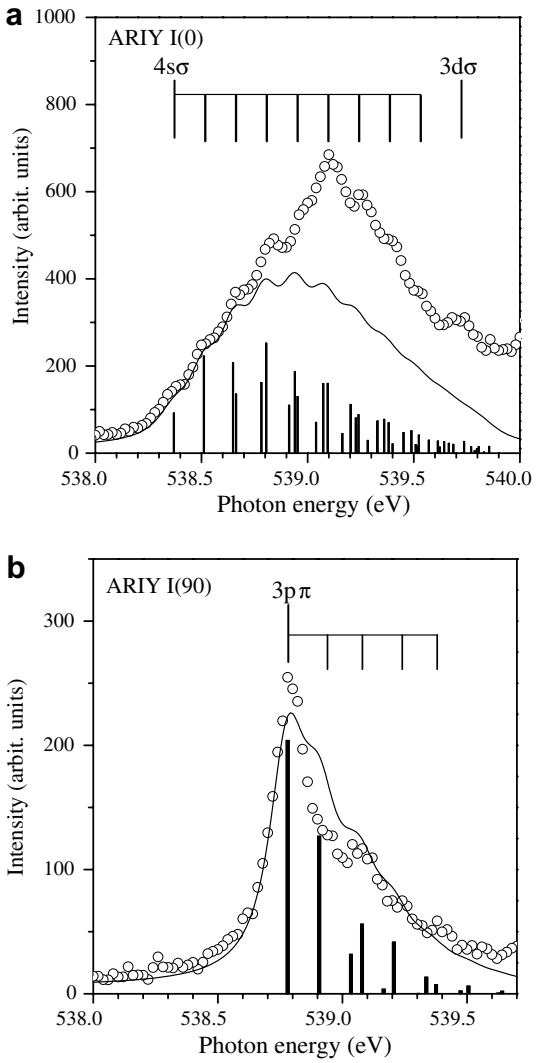

Fig. 3. Vibrationally resolved spectra of the (a) O $1s^{-1}4s\sigma$ and (b) O $1s^{-1}3p\pi$ state of N_2O in comparison to our numerical results. Teeth of the comb represent the vibrational components experimentally observed (cf. Table 1). The theoretical spectra are shown as vertical solid lines (cf. Table 1); only the 4sσ spectrum is included in (a). The solid curve corresponds to the sum of the individual components after convolution with a Voigt function with a Lorentzian width of 160 meV and a Gaussian width of 50 meV.

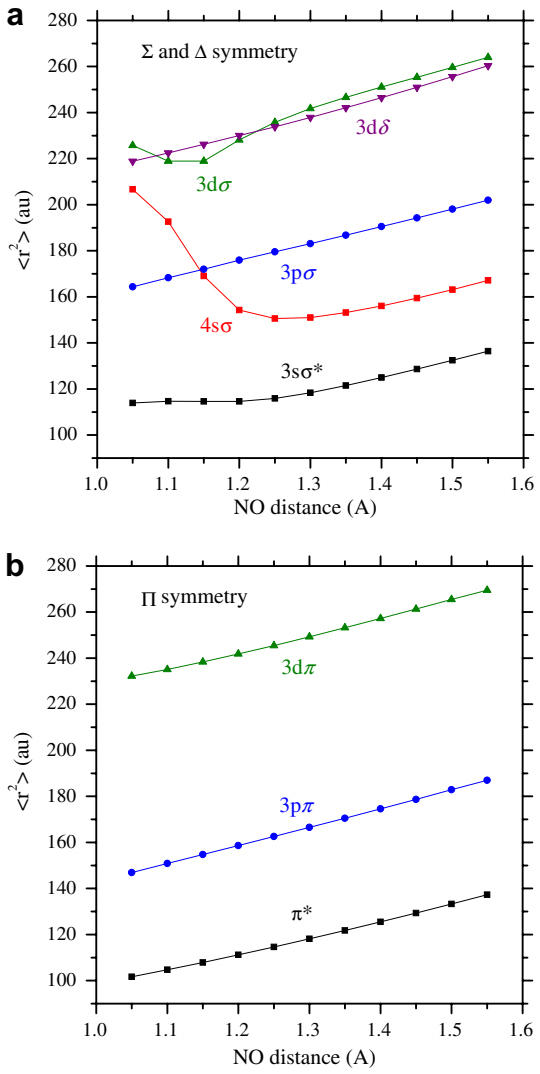

Fig. 4. Second moments of the low-lying O 1s excited states in (a) Σ-, Δ- and (b) Π-symmetry with the cut of $R_{NN} = 1.10$ Å. Curves are shown for the diabatic states.

the valence mixing, we have calculated the electronic part of the second moments $\langle r^2\rangle = \langle x^2\rangle + \langle y^2\rangle + \langle z^2\rangle$. The $\langle r^2\rangle$ values represent the distributions of total electrons and therefore sensitively reflect the character of the excited states discussed here. The values obtained for the states of interest are plotted in Fig. 4. The values for $nl\pi$ represent the unperturbed Rydberg character and thus can be used as reference. We notice that the values are very similar for π^* and 3sσ, indicating that 3sσ is very much valence-like. We also notice that the value of 4sσ varies rapidly as a function of NO distances and becomes much smaller than those for unperturbed 3pσ and 3pπ, illustrating that the valence character enhances at NO distances above ~1.15 Å where the excitation takes place (~1.185 Å). 3dσ is also perturbed but the valence mixing is less significant and localized at ~1.15 Å.

5. Summary

We have measured angle-resolved energetic-ion yield spectra in the region of the O 1s excitation of N_2O and obtained absorption spectra of Σ- and Π-symmetries. The vibrational excitations are found to be specific to the individual Rydberg states in the Σ-symmetry spectrum. We have carried out *ab initio* calculations for two-dimensional potential energy surfaces of the ground and O 1s core-excited states. The Franck–Condon analysis based on the *ab initio* potential energy surfaces reproduces well the observed state-specificity of vibrational excitations. The irregular vibrational excitations along the same *n*sσ Rydberg series are attributed the valence-Rydberg coupling in light of the second moment analysis.

Acknowledgements

The experiment was carried out with the approval of the SPring-8 program review committee. This study was supported by Grants-in-Aid for Scientific Research from the Japanese Society for the Promotion of Science (JSPS) and a Grant for Creative Scientific Research from the Ministry of Education, Science, Culture, and Sports of Japan. RF acknowledges the Swedish Research Council (VR) and Tohoku University for hospitality and financial support during his stay there.

References

[1] A.P. Hitchcock, Phys. Scr. T31 (1990) 159.
[2] K. Ueda, J. Phys. B: At. Mol. Opt. Phys. 36 (2003) R1.
[3] N. Saito, I.H. Suzuki, Phys. Rev. Lett. 61 (1988) 2740.
[4] A. Yagishita, H. Maezawa, M. Ukai, E. Shigemasa, Phys. Rev. Lett. 62 (1989) 36.
[5] K. Lee, D.Y. Kim, C.I. Ma, D.A. Lapiano-Smith, D.M. Hanson, J. Chem. Phys. 93 (1990) 7936.
[6] E. Shigemasa, K. Ueda, Y. Sato, T. Sasaki, A. Yagishita, Phys. Rev. A 45 (1992) 2915.
[7] R.N. Zare, Mol. Photochem. 4 (1972) 1.
[8] G.E. Busch, K.R. Wilson, J. Chem. Phys. 56 (1972) 3638.
[9] J. Adachi, N. Kosugi, A. Yagishita, J. Phys. B: At. Mol. Opt. Phys. 38 (2005) R127.
[10] J. Adachi, N. Kosugi, E. Shigemasa, A. Yagishita, J. Chem. Phys. 102 (1995) 7369.
[11] T. Tanaka et al., Chem. Phys. Lett. 428 (2006) 34.
[12] K.C. Prince, L. Avaldi, M. Coreno, R. Camilloni, M. de Simone, J. Phys. B: At. Mol. Opt. Phys. 32 (1999) 2551.
[13] H. Nakatsuji, Chem. Phys. Lett. 59 (1978) 362.
[14] H. Nakatsuji, Chem. Phys. Lett. 67 (1979) 329.
[15] H. Nakatsuji, Chem. Phys. Lett. 177 (1991) 331.
[16] H. Nakatsuji, Computational Chemistry – Review of Current Trends, vol. 2, World Scientific, 1997.
[17] M. Ehara, J. Hasegawa, H. Nakatsuji, SAC–CI Method Applied to Molecular Spectroscopy, in: C.E. Dykstra, G. Frenking, K.S. Kim, G.E. Scuseria (Eds.), Theory and Applications of Computational Chemistry: The First 40 Years, Elsevier, Oxford, 2005, p. 1099.
[18] R.W. Shaw Jr., T.D. Thomas, Chem. Phys. Lett. 22 (1973) 127.
[19] A.P. Hitchcock, C.E. Brion, J. Phys. B14 (1981) 4399.
[20] T.D. Thomas, L.J. Sæthre, S.L. Sorensen, S. Svensson, J. Chem. Phys. 109 (1998) 1041.
[21] M.N.R. Wohlfahrth, L.S. Cederbaum, J. Chem. Phys. 116 (2002) 8723.
[22] H. Ohashi et al., Nucl. Instr. Methods A 467–468 (2001) 529.
[23] H. Ohashi et al., Nucl. Instr. Methods A 467–468 (2001) 533.
[24] T. Tanaka, H. Kitamura, J. Synchrotron Radiat. 3 (1996) 47.
[25] N. Saito et al., Phys. Rev. A 62 (2000) 042503.
[26] J.L. Teffo, A. Chedin, J. Mol. Spectrosc. 135 (1989) 389.
[27] T.H. Dunning Jr., J. Chem. Phys. 90 (1989) 1007.
[28] K. Kaufmann, C. Nager, M. Jungen, Chem. Phys. 95 (1985) 385.
[29] R. Fukuda, H. Nakatsuji, submitted for publication.
[30] H. Nakatsuji, Chem. Phys. 75 (1983) 425.
[31] M.J. Frisch et al., Gaussian Development Version, Revision E.05, Gaussian, Inc., Wallingford CT, 2006.